Computers and Structures 202 (2018) 15–24

Contents lists available at ScienceDirect

Computers and Structures

journal homepage: www.elsevier.com/locate/compstruc

Further insights into an implicit time integration scheme for structural dynamics

Gunwoo Noh [a], Klaus-Jürgen Bathe [b,*]

[a] Kyungpook National University, Daegu 41566, Republic of Korea
[b] Massachusetts Institute of Technology, Cambridge, MA 02139, USA

ARTICLE INFO

Article history:
Received 31 October 2017
Accepted 12 February 2018

Keywords:
Dynamics
Finite element solutions
Direct time integrations
Implicit and explicit schemes
Stability and accuracy
Bathe method

ABSTRACT

The objective in this paper is to present some new insights into an implicit direct time integration scheme, the Bathe method, for the solution of the finite element equations of structural dynamics. The insights pertain to the use of the parameters in the method, and in particular the value of the time step splitting ratio. We show that with appropriate values of this ratio large amplitude decays can be obtained as may be desirable in some solutions. We give the theoretical analysis of the method for the parameters used, including for very large time steps, and illustrate numerically the new insights gained.

1. Introduction

The finite element method is now quite widely used for the solution of structural vibrations and wave propagations. For such solutions, methods of direct time integration of the governing finite element equations are frequently used. When so done, for wave propagation analyses, mostly explicit schemes are employed, while for structural vibration solutions mostly implicit schemes are used [1]. While such use is still mostly the case, lately implicit schemes are also increasingly being employed to solve wave propagation problems.

An important characteristic of an implicit direct time integration scheme is that it can be unconditionally stable, which means that the time step Δt can be selected solely based on accuracy considerations. For the solution of the finite element structural dynamics equations, a frequently used scheme is the trapezoidal rule, a special case of the Newmark method [1,2]. Some other techniques are, for example, the Wilson method [1,3,4], the methods discussed by Zhou and Tamma [5], and the three parameter method [6–8]. More recently, the Bathe method has been proposed and has attracted significant attention and use [9–11].

The Bathe method is a composite scheme using two sub-steps per time step Δt, but *the method is used like a single-step method with some intermediate calculations*. These, however, make the method about twice as expensive as the trapezoidal rule per time step Δt. Since there seems to be a considerable extra cost compared to using other methods, an analyst may question why to use this method. The advantages are much better accuracy characteristics allowing larger time steps in the integration and, overall, the more effective solution of linear and nonlinear problems. The method is now widely used for structural analyses and fluid-structure interactions, see e.g., Refs. [12,13].

The objective in this paper is to focus on some considerations regarding the method, observations and insights that are related to what we have learned since the first publication of the method. The new insights are based on our latest experiences and thoughts spurred by other publications [13–21]. Hence, this paper might be viewed as a continuation of Ref. [11].

In the next section, we briefly summarize the basic equations of the Bathe method. As originally published, there are three parameters (α, δ, γ) that can be set. Although it is in practical analyses frequently best to simply use the defaults of these parameters, as emphasized in Refs. [10,11], it is important to realize that, if desired, the three parameters can of course be changed by the analyst. Of particular interest are the properties when γ is changed. We therefore discuss, in Sections 3 and 4, the stability and accuracy of the method when changing γ, where we include the use of γ larger than 1.0 and large time step to period ratios. Finally, in Section 5, we present our concluding remarks.

* Corresponding author.
E-mail address: kjb@mit.edu (K.J. Bathe).

https://doi.org/10.1016/j.compstruc.2018.02.007
0045-7949/

2. The basic equations of the Bathe time integration scheme

To provide a basis for our discussion, we summarize here briefly the governing equations of the Bathe method [9–11]. In the procedure, we calculate the unknown displacements, velocities, and accelerations by considering the time step Δt to consist of two sub-steps. The sub-step sizes are $\gamma\Delta t$ and $(1-\gamma)\Delta t$ for the first and second sub-steps, respectively. Of course, in principle more sub-steps could be employed, see for example Ref. [9].

In the Bathe method, well-known integration schemes are used for each sub-step [10]. In the first sub-step, we utilize the trapezoidal rule, or more generally, the Newmark method

$$^{t+\gamma\Delta t}\dot{\mathbf{U}} = {}^{t}\dot{\mathbf{U}} + [(1-\delta)\,{}^{t}\ddot{\mathbf{U}} + \delta\,{}^{t+\gamma\Delta t}\ddot{\mathbf{U}}]\gamma\Delta t \tag{1}$$

$$^{t+\gamma\Delta t}\mathbf{U} = {}^{t}\mathbf{U} + {}^{t}\dot{\mathbf{U}}\gamma\Delta t + \left[\left(\frac{1}{2}-\alpha\right){}^{t}\ddot{\mathbf{U}} + \alpha\,{}^{t+\gamma\Delta t}\ddot{\mathbf{U}}\right]\gamma^2\Delta t^2 \tag{2}$$

and in the second sub-step, we utilize the Euler 3-point backward rule

$$^{t+\Delta t}\dot{\mathbf{U}} = c_1\,{}^{t}\mathbf{U} + c_2\,{}^{t+\gamma\Delta t}\mathbf{U} + c_3\,{}^{t+\Delta t}\mathbf{U} \tag{3}$$

$$^{t+\Delta t}\ddot{\mathbf{U}} = c_1\,{}^{t}\dot{\mathbf{U}} + c_2\,{}^{t+\gamma\Delta t}\dot{\mathbf{U}} + c_3\,{}^{t+\Delta t}\dot{\mathbf{U}} \tag{4}$$

where

$$c_1 = \frac{1-\gamma}{\gamma\Delta t},\quad c_2 = \frac{-1}{(1-\gamma)\gamma\Delta t},\quad c_3 = \frac{2-\gamma}{(1-\gamma)\Delta t} \tag{5}$$

Considering linear analysis, the equilibrium equations applied at time $t+\gamma\Delta t$ and time $t+\Delta t$ are

$$\mathbf{M}\,{}^{t+\gamma\Delta t}\ddot{\mathbf{U}} + \mathbf{C}\,{}^{t+\gamma\Delta t}\dot{\mathbf{U}} + \mathbf{K}\,{}^{t+\gamma\Delta t}\mathbf{U} = {}^{t+\gamma\Delta t}\mathbf{R} \tag{6}$$

$$\mathbf{M}\,{}^{t+\Delta t}\ddot{\mathbf{U}} + \mathbf{C}\,{}^{t+\Delta t}\dot{\mathbf{U}} + \mathbf{K}\,{}^{t+\Delta t}\mathbf{U} = {}^{t+\Delta t}\mathbf{R} \tag{7}$$

where **M**, **C**, **K** are the mass, damping and stiffness matrices, and the vectors **U** and **R** list, respectively, the nodal displacements (rotations) and externally applied nodal forces (moments). An overdot denotes a time derivative. Using the relations in Eqs. (1)–(5) with the equilibrium equations at the two time points, Eqs. (6) and (7), we construct the time-stepping equations as

$$\hat{\mathbf{K}}_1\,{}^{t+\gamma\Delta t}\mathbf{U} = \hat{\mathbf{R}}_1 \tag{8}$$

$$\hat{\mathbf{K}}_2\,{}^{t+\Delta t}\mathbf{U} = \hat{\mathbf{R}}_2 \tag{9}$$

where

$$\hat{\mathbf{K}}_1 = \frac{1}{\alpha\gamma^2\Delta t^2}\mathbf{M} + \frac{\delta}{\alpha\gamma\Delta t}\mathbf{C} + \mathbf{K} \tag{10}$$

$$\hat{\mathbf{K}}_2 = c_3{}^2\mathbf{M} + c_3\mathbf{C} + \mathbf{K} \tag{11}$$

$$\begin{aligned}\hat{\mathbf{R}}_1 = {}&{}^{t+\gamma\Delta t}\mathbf{R} + \mathbf{M}\left(\left(\frac{1}{2\alpha}-1\right){}^{t}\ddot{\mathbf{U}} + \frac{1}{\alpha\gamma\Delta t}{}^{t}\dot{\mathbf{U}} + \frac{1}{\alpha\gamma^2\Delta t^2}{}^{t}\mathbf{U}\right)\\ &+ \mathbf{C}\left(\frac{(\delta-2\alpha)\gamma\Delta t}{2\alpha}{}^{t}\ddot{\mathbf{U}} + \left(\frac{\delta}{\alpha}-1\right){}^{t}\dot{\mathbf{U}} + \frac{\delta}{\alpha\gamma\Delta t}{}^{t}\mathbf{U}\right)\end{aligned} \tag{12}$$

$$\begin{aligned}\hat{\mathbf{R}}_2 = {}&{}^{t+\Delta t}\mathbf{R} - \mathbf{M}(c_1c_3\,{}^{t}\mathbf{U} + c_2c_3\,{}^{t+\gamma\Delta t}\mathbf{U} + c_1\,{}^{t}\dot{\mathbf{U}} + c_2\,{}^{t+\gamma\Delta t}\dot{\mathbf{U}})\\ &- \mathbf{C}(c_1\,{}^{t}\mathbf{U} + c_2\,{}^{t+\gamma\Delta t}\mathbf{U})\end{aligned} \tag{13}$$

While the case of the trapezoidal rule ($\alpha = 1/4, \delta = 1/2$) as the first sub-step with $\gamma = 1/2$ (or $\gamma = 2-\sqrt{2}$) has been mostly used and analyzed, in principle, α and δ in the Newmark method and γ in the composite scheme can be chosen. Hence we can interpret the scheme as a "quite general time stepping technique."

To have a second-order accurate composite procedure with the second-order accurate Euler 3-point backward rule for the second sub-step, it is apparent that the scheme in the first sub-step should have at least second-order accuracy. Hence in the Newmark method used in the Bathe scheme, δ must be equal to 1/2, which gives second-order accuracy of the displacements, velocities and accelerations and also no dissipation. This has been proven explicitly in Ref. [20]. However, not seeking second-order accuracy and choosing other values of δ, we may well have that with some values of δ, α and γ good solution accuracy for some problems is achieved. This approach may be valuable to obtain problem-fitted accuracy characteristics (e.g. larger numerical dissipation).

Considering nonlinear analysis, for some specific nonlinear problems, the parameters $\gamma = 0.73$, $\alpha = 1/4$ and $\delta = 1/2$ were identified to be suitable [17]. Also, for two nonlinear problems, the effect of choosing different values of γ with $\alpha = 1/4$ and $\delta = 1/2$ has been briefly studied in Ref. [16], and it was found that the use of different sets of parameters for different classes of nonlinear problems will likely yield a near-optimal time stepping measured on computational cost. However, to identify these sets of optimal parameters requires considerable analysis and experimentation. On the other hand, the insights that we can gain in linear analysis are also very useful for obtaining effective solutions in nonlinear analysis.

Note that the splitting ratio, γ, has been set to $\gamma \in (0,1)$ in the analysis and use of the Bathe method, as referred to above, and in the development of a new scheme based on the Bathe composite strategy [14,18,19,21]. However, in principle, the value of γ can also be defined in a larger range. In the following sections, we therefore also study the stability and accuracy of the method allowing γ to be greater than 1. Using γ greater than 1 is quite different from using θ greater than 1 in the Wilson method, because in the Bathe method the equilibrium equations are satisfied at both time points considered, see Eqs. (6) and (7).

3. Stability and accuracy of the Bathe method

In the decoupled modal equations, the method may be expressed as [1]

$$\begin{bmatrix} {}^{t+\Delta t}\ddot{x} \\ {}^{t+\Delta t}\dot{x} \\ {}^{t+\Delta t}x \end{bmatrix} = \mathbf{A}\begin{bmatrix} {}^{t}\ddot{x} \\ {}^{t}\dot{x} \\ {}^{t}x \end{bmatrix} + \mathbf{L_a}\,{}^{t+\gamma\Delta t}r + \mathbf{L_b}\,{}^{t+\Delta t}r \tag{14}$$

where $\mathbf{A}$, $\mathbf{L_a}$ and $\mathbf{L_b}$ are the integration approximation and load operators, respectively, and x and an overdot denote the displacement in the modal space and a time derivative, respectively (see Appendix A). The stability and some accuracy characteristics of the method may be studied using this form of the scheme.

Focusing on the case of no physical damping, the characteristic polynomial of $\mathbf{A}$ is

$$p(\lambda) = \lambda^3 - 2A_1\lambda^2 + A_2\lambda - A_3 \tag{15}$$

where

$$\begin{aligned} A_1 &= \frac{1}{\beta_{01}\beta_{02}}\left(\begin{matrix}(1/4)\gamma^2(2\alpha-\delta)(\gamma-1)\Omega_0^4\\ +\left(\begin{matrix}-1+\gamma^4\alpha-4\gamma^3\alpha+(1/4)(16\alpha+2\delta+1)\gamma^2\\ +(1/4)(-4\delta+2)\gamma\end{matrix}\right)\Omega_0^2+(\gamma-2)^2\end{matrix}\right);\\ A_2 &= \frac{1}{\beta_{01}\beta_{02}}\left(\left(\begin{matrix}\gamma^4\alpha-4\gamma^3\alpha+(1/2)(8\alpha+2\delta+1)\gamma^2\\ +(1/2)(-4\delta-2)\gamma+1\end{matrix}\right)\Omega_0^2+(\gamma-2)^2\right);\\ A_3 &= 0; \end{aligned} \tag{16}$$

$$\beta_{01} = \Omega_0^2\alpha\gamma^2 + 1;\quad \beta_{02} = (\gamma-1)^2\Omega_0^2 + (\gamma-2)^2$$

where ω_0 is the modal natural frequency and $\Omega_0 = \omega_0 \Delta t$.

To represent oscillatory solutions, the eigenvalues of **A** should remain in the complex plane. Since A_3 = 0, we have a zero eigenvalue and two non-zero eigenvalues.

The condition for the eigenvalues to be complex conjugate for all positive Ω_0 gives

$$\delta = 2\alpha; \quad \alpha > 0 \tag{17}$$

with the additional condition –

either

$$b_2 > 0; \quad b_2^2 - 4b_1 b_3 \leqslant 0 \tag{18}$$

or

$$b_2 \leqslant 0 \tag{19}$$

where

$$b_1 = -\gamma^2(\gamma^2 - 2\gamma + 2)\left(\gamma^2\alpha - 2\alpha\gamma + \frac{1}{2}\right)\alpha(\gamma - 1)^2; \tag{20}$$

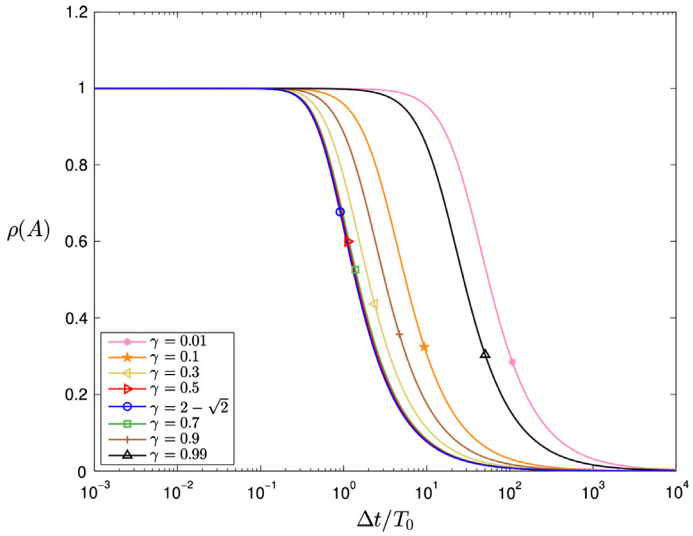

(a) Spectral radii of approximation operator of the Bathe method when $\xi = 0$ for various values of $\gamma \in (0,1)$ with $\alpha = 1/4$ and $\delta = 1/2$.

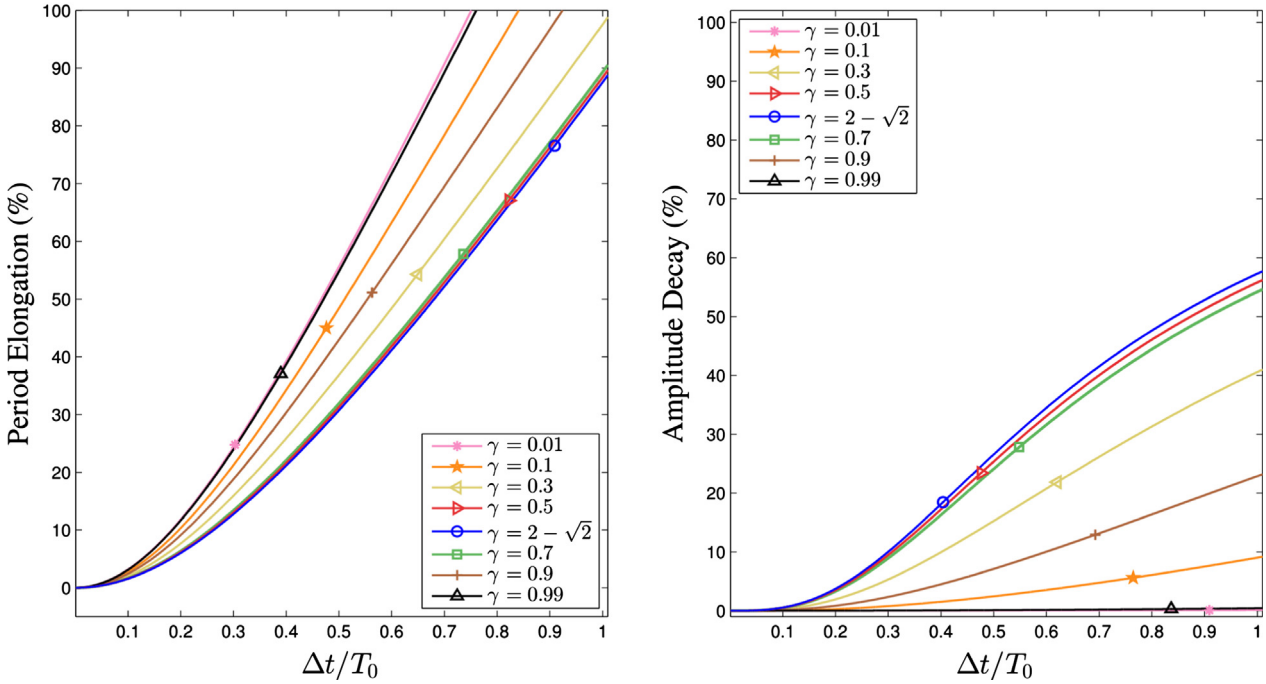

(b) Percentage period elongations and amplitude decays of the Bathe method when $\xi = 0$ for various values of $\gamma \in (0,1)$ with $\alpha = 1/4$ and $\delta = 1/2$.

Fig. 1. The Bathe method for various values of γ with $\alpha = 1/4$ and $\delta = 1/2$.

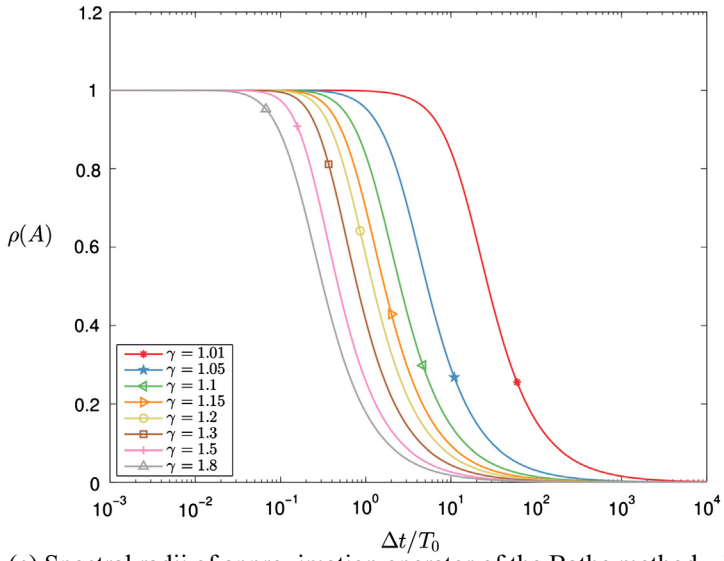

(c) Spectral radii of approximation operator of the Bathe method when $\xi = 0$ for various values of $\gamma > 1$ with $\alpha = 1/4$ and $\delta = 1/2$.

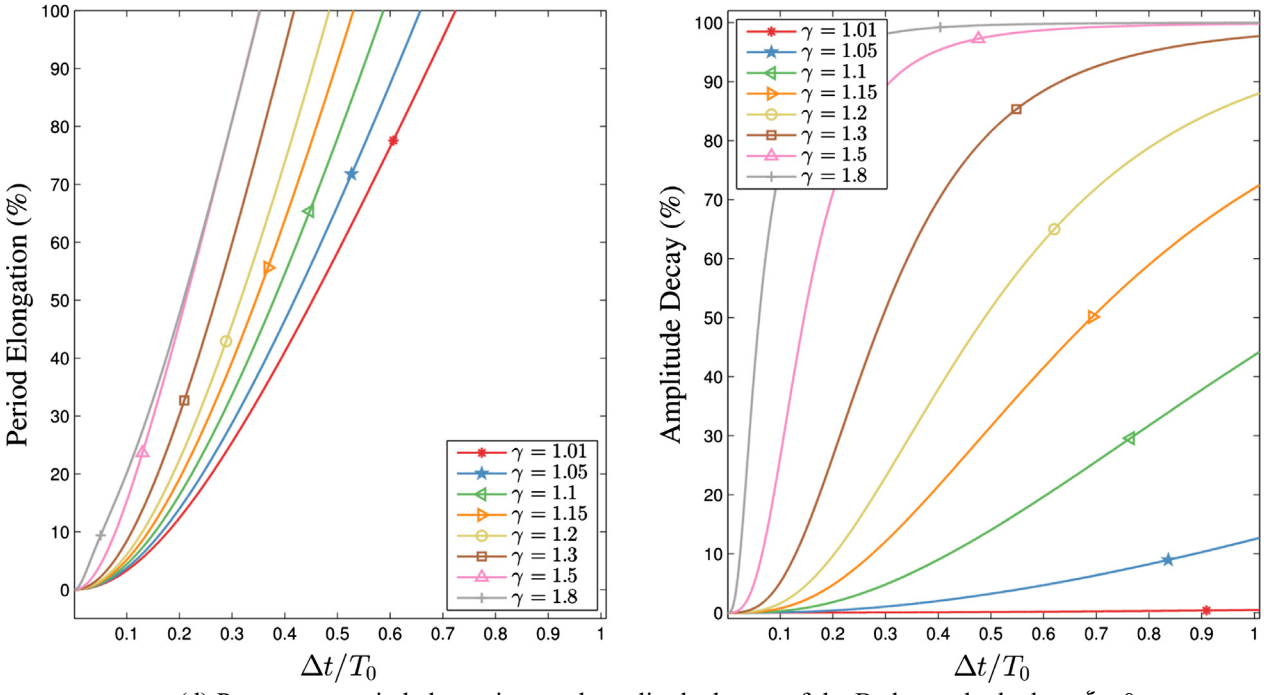

(d) Percentage period elongations and amplitude decays of the Bathe method when $\xi = 0$ for various values of $\gamma > 1$ with $\alpha = 1/4$ and $\delta = 1/2$.

Fig. 1 (*continued*)

$$b_2 = -2\gamma(\gamma-2)^2\left(\gamma^3\alpha - 3\gamma^2\alpha + \left(-\frac{1}{2}\alpha^2 + \frac{13\alpha}{4} + \frac{7}{32}\right)\gamma - \alpha - \frac{1}{4}\right); \tag{21}$$

$$b_3 = -\gamma^4 + 8\gamma^3 - 24\gamma^2 + 32\gamma - 16 \tag{22}$$

Using the Routh-Hurwitz stability criteria for Eq. (15) with the relations in Eqs. (17)–(19), we obtain the useful relation for unconditional stability and oscillatory solutions:

$$\delta = \frac{1}{2}; \alpha = \frac{1}{4}; \{\gamma \in \mathbb{R} | \gamma \neq 0, \gamma \neq 1\} \tag{23}$$

Note that $\gamma = 0$ and $\gamma = 1$ should be avoided in practice since we would have γ and $(1-\gamma)$ in the denominators of constants in the method. Also, there are other values of δ, α and γ for unconditional stability, but for values other than $\delta = 1/2$ and $\alpha = 1/4$, the range of γ for unconditional stability is severely reduced. With $\delta = 1/2$ and $\alpha = 1/4$ we have $b_2^2 - 4b_1b_3 = 0$ for all γ; therefore

the values in Eq. (23) render the method unconditionally stable and the principal roots of the integration approximation operator, **A**, to be complex conjugate.

Since the principal roots remain in the complex plane for all positive Ω_0, the spectral radius, $\rho(\mathbf{A})$, becomes

$$\rho(\mathbf{A}) = \sqrt{A_2} \tag{24}$$

Fig. 1 shows the spectral radii and the period elongations and amplitude decays for various values of γ with $\alpha = 1/4$ and $\delta = 1/2$, including when γ is greater than 1.0. The spectral radius expressed in Eq. (24) with $\alpha = 1/4$ and $\delta = 1/2$ has a local minimum at $\gamma = 2 - \sqrt{2}$ (within the range $0 < \gamma < 1$) and this splitting ratio provides maximum amplitude decay with minimum period elongation when $\gamma \in (0, 1)$, which was already reported [11,17,19,20,22,23]. These curves are quite close to those using $\gamma = 0.5$.

Indeed, the spectral properties of the Bathe method with $\alpha = 1/4$ and $\delta = 1/2$ possess a symmetry (with some scaling) with the center of $\gamma = 2 - \sqrt{2}$, namely γ and $2(1-\gamma)/(2-\gamma)$ provide identical spectral properties, see Fig. 2. That is, γ and $2(1-\gamma)/(2-\gamma)$ give the same characteristic polynomial in Eq. (15). Hence, the spectral properties of $\gamma \in (0, 2-\sqrt{2})$ can be reproduced by using $\gamma \in (2-\sqrt{2}, 1)$, where γ in the range of $(1, 2)$ has its counterpart in $(-\infty, 0)$.

Considering Fig. 1, the curves calculated for $2(1-\gamma)/(2-\gamma)$ are therefore identical to those given for γ, that is, for example, the results obtained with $\gamma = 0.1$ are also the results using $\gamma = 0.9474$ (the value is rounded). As a result, we can see that the amplitude decay and period elongation curves for γ approaching 0.0 and 1.0 (from $\gamma = 2 - \sqrt{2}$) behave similarly, that is, the curves approach those of the trapezoidal rule. This behavior is also reflected in the value of the spectral radius as a function of $\Delta t/T_0$.

We also have that the results obtained with $\gamma = 1.01$ are also the results using $\gamma = -.0202$. However, a negative γ value requires the use of the equilibrium equations at $t < 0$, which is undesirable, clearly for the first time step. Therefore, while the same spectral properties arise, positive values of γ are preferred.

While with $\gamma \in (0, 1)$ less numerical dissipation occurs as γ decreases or increases from $2 - \sqrt{2}$, we have that for $\gamma \in (1, \infty)$ the amount of numerical dissipation increases from zero as γ increases. Here correspondingly, the range over which the spectral radius as a function of $\Delta t/T_0$ is equal to 1.0 decreases. On the other hand, the period elongation increases as γ decreases or increases from $2 - \sqrt{2}$ with $\gamma \in (0, 1)$ and the period elongation increases as γ increases for $\gamma \in (1, \infty)$. Comparing the results, we observe for example that $\gamma = 1.15$ provides a similar spectral radius curve as $\gamma = 2 - \sqrt{2}$ but corresponds to a much larger period elongation.

Finally, we note that larger values of γ within $\gamma \in (1, \infty)$ result in significant numerical dissipation which may be useful for specific problem solutions.

To compare with some other methods, Fig. 3 shows the spectral radii and accuracy characteristics of various schemes mentioned in Section 1.

4. Accuracy in large time steps

To address the accuracy characteristics of a time integration method, the period elongation and amplitude decay seen in the solution of a single-degree of freedom oscillator have been widely used. These properties result into numerical dispersion and dissipation, respectively, when considering the solutions of finite element equations. While the basic concepts were used in early work [4,24], more detailed definitions and the way of calculating these measures were later introduced, see Ref. [15] and the references therein.

We consider the free motion of a single degree of freedom system with the exact solution

$$u_e = e^{-\xi\omega_0 t}(c_1 \cos(\omega_d t) + c_2 \sin(\omega_d t)) \tag{25}$$

where ξ is the damping ratio, $\omega_d = \omega_0\sqrt{1-\xi^2}$, and the parameters c_1 and c_2 are determined by the initial displacement d_0 and the initial velocity v_0 as $c_1 = d_0$ and $c_2 = (1/\omega_d)(\xi\omega_0 d_0 + v_0)$.

The numerical solution by a time integration method using Eq. (14), that is, ${}^t\mathbf{X} = [{}^t\ddot{x};\ {}^t\dot{x};\ {}^t x]$, can be expressed as

$${}^{n\Delta t}\mathbf{X} = \hat{\mathbf{c}}_1\lambda_1^n + \hat{\mathbf{c}}_2\lambda_2^n + \hat{\mathbf{c}}_3\lambda_3^n \tag{26}$$

where the parameter vectors, $\hat{\mathbf{c}}_i$, are determined by the initial conditions and the eigenvectors $\boldsymbol{\psi}_i$ as

$$\hat{\mathbf{c}}_i = \boldsymbol{\psi}_i z_i \tag{27}$$

$$[z_1\ z_2\ z_3]^{\mathrm{T}} = [\boldsymbol{\psi}_1\ \boldsymbol{\psi}_2\ \boldsymbol{\psi}_3]^{-1}\mathbf{X}_0 \tag{28}$$

Note that any values seen as errors in $\hat{\mathbf{c}}_i$ mainly affect the numerical solution in the first few steps while the spectral properties of the time integration method determine the long-term solution.

Since the spurious root, λ_3, satisfies the condition $|\lambda_3| < |\lambda_{1,2}|$, the numerical solution can be expressed as

$${}^{n\Delta t}\mathbf{X} = e^{-\bar{\xi}\bar{\Omega}_d n}(\bar{\mathbf{c}}_1 \cos(\bar{\Omega}_d n) + \bar{\mathbf{c}}_2 \sin(\bar{\Omega}_d n)) + \bar{\mathbf{c}}_3\lambda_3 \tag{29}$$

where $\bar{\Omega}_d = \bar{\omega}_d\Delta t$ with $\bar{\omega}_d$ being the "numerical natural frequency", and $\bar{\mathbf{c}}_3 = \hat{\mathbf{c}}_3$,

$$\lambda_{1,2} = \left(\sqrt{A_2}, \pm\bar{\Omega}_d\right) \tag{30}$$

in polar coordinates, such that

$$\frac{\partial(\bar{\Omega}_d)}{\partial(\Delta t)} \geqslant 0 \quad \text{for } \Delta t \geqslant 0 \tag{31}$$

and

$$\bar{\xi} = -\frac{1}{2\Omega_0}\ln(A_2) = -\frac{1}{\Omega_0}\ln(\rho(\mathbf{A})) \tag{32}$$

and the parameter vectors of interest are determined as $\bar{\mathbf{c}}_1 = \mathrm{Re}(\hat{\mathbf{c}}_1 + \hat{\mathbf{c}}_2)$ and $\bar{\mathbf{c}}_2 = \mathrm{Re}(i(\hat{\mathbf{c}}_1 - \hat{\mathbf{c}}_2))$ in which i is the imaginary unit.

The period elongation, PE, is then defined using $\bar{\Omega}_d$ as

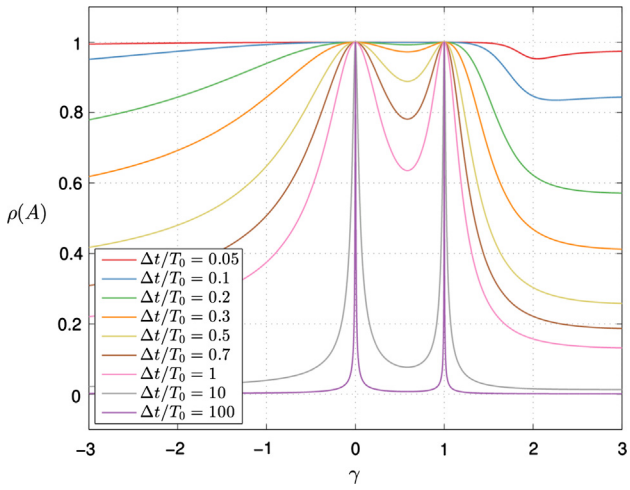

Fig. 2. Spectral radii of approximation operator of the Bathe method when $\xi = 0$, for various values of γ with $\alpha = 1/4$ and $\delta = 1/2$.

$$PE = \frac{\bar{T}_d - T_0}{T_0} = \frac{\Omega_0}{\bar{\Omega}_d} - 1 \tag{33}$$

Using Eq. (29) with the solution at time $\bar{T}_d$, the "numerical natural period", we obtain the expression for the amplitude decay, AD, as

$$AD = 1 - \exp\left(-2\pi\bar{\xi}\frac{\Omega_0}{\bar{\Omega}_d}\right) \tag{34}$$

Of course, the frequently used approximate expression $AD_{approx} = 2\pi\bar{\xi}$, is recovered by taking the Taylor expansion on Eq. (34) for small $\bar{\xi}$. The two expressions provide similar results for a small AD, while the difference might not be negligible for cases of larger time steps used.

With the expressions in Eqs. (30)–(34), we are able to calculate the period elongation and the amplitude decay only with A_1 and A_2,

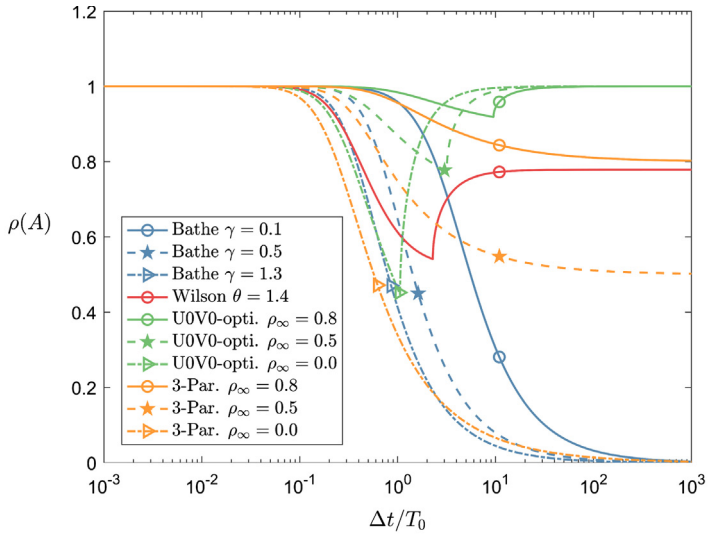

(a) Spectral radii of approximation operator when $\xi = 0$

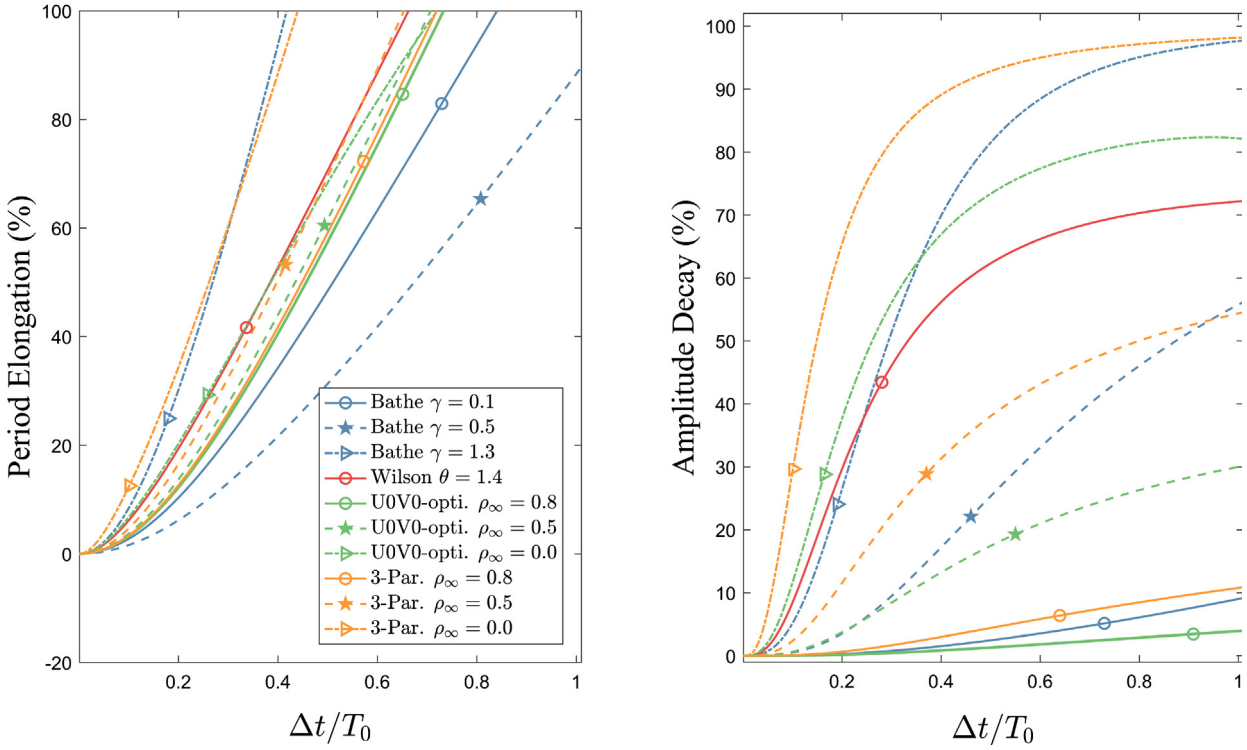

(b) Percentage period elongations and amplitude decays when $\xi = 0$

Fig. 3. Spectral radii, period elongations and amplitude decays of various methods. For the Bathe method $\alpha = 1/4$ and $\delta = 1/2$ are used. The U0V0 method is described in Ref. [5] and the 3-Par. method is described in Refs. [6–8].

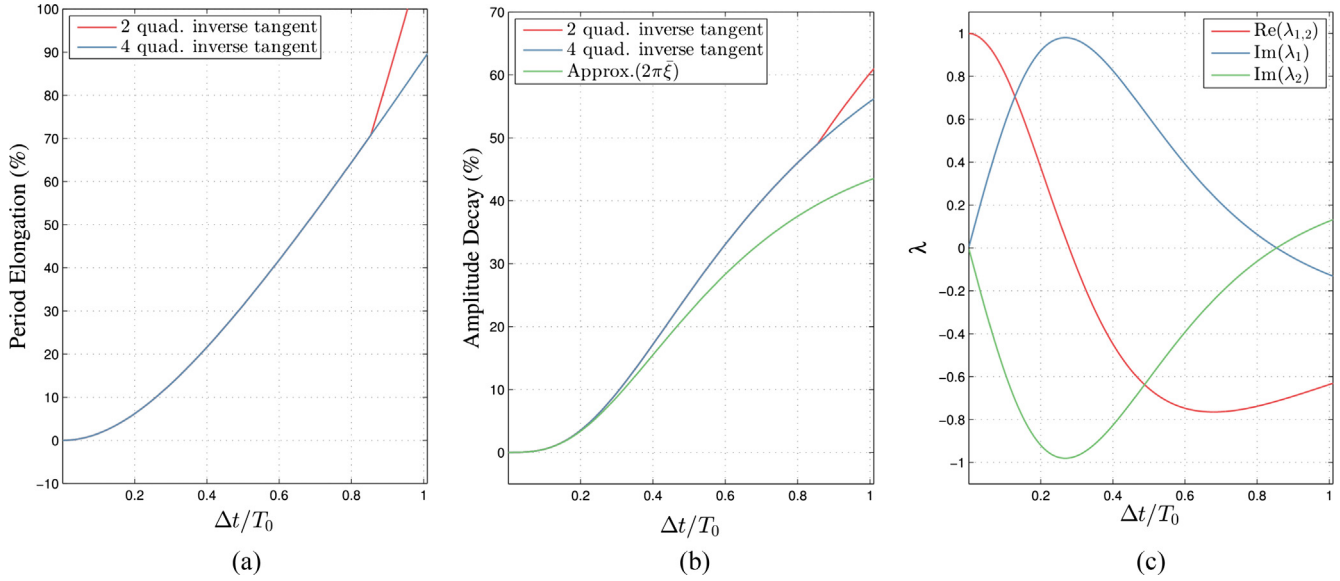

Fig. 4. Bathe method with $\alpha = 1/4, \delta = 1/2, \gamma = 1/2$. (a) Period elongations calculated using 2 quadrant inverse tangent $\left(\theta = \tan^{-1}\left(\sqrt{A_2 - A_1^2}/A_1\right)\right)$ and 4 quadrant inverse tangent (Eq. (36)). (b) Amplitude decays calculated using 2 quad. inverse tangent, 4 quad. tangent and approximate expression $(2\pi\bar{\xi})$. (c) Eigenvalues used in the calculation of 4 quad. inverse tangent.

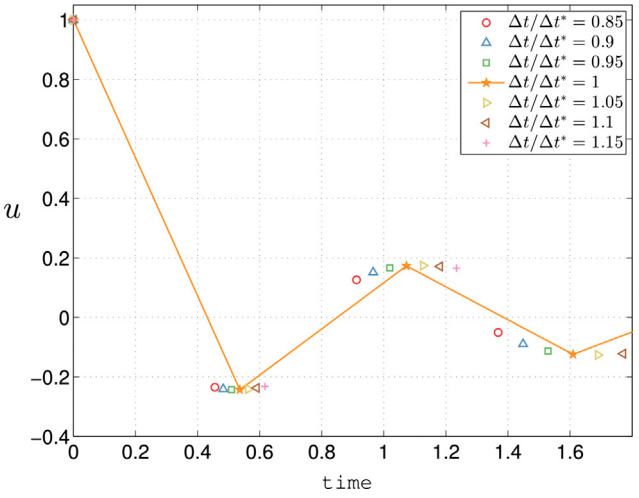

Fig. 5. Numerical results of the single degree of freedom system described by Eq. (37) using the Bathe method with $\alpha = 1/4, \delta = 1/2, \gamma = 1/2$ for various time step sizes; $\Delta t^*/T_0 \simeq 0.854$.

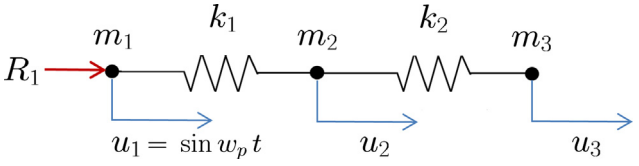

Fig. 6. Model problem of three degrees of freedom spring system, $k_1 = 10^7, k_2 = 1, m_1 = 0, m_2 = 1, m_3 = 1, \omega_p = 1.2$.

which are given in Eq. (16) for the Bathe method; we do not need any numerical fitting which was frequently used in earlier works.

Let us now consider $\bar{\Omega}_d$ in Eq. (30) for the calculation of PE and AD with larger time steps. Since the two nonzero eigenvalues of Eq. (15) are complex conjugates, we may define the first eigenvalue as the one rotating counter-clockwise and the second eigenvalue as the one rotating clockwise as in Eqs. (30) and (31); thus we here define $\bar{\Omega}_d$ as a "four" quadrant inverse tangent of the eigenvalue

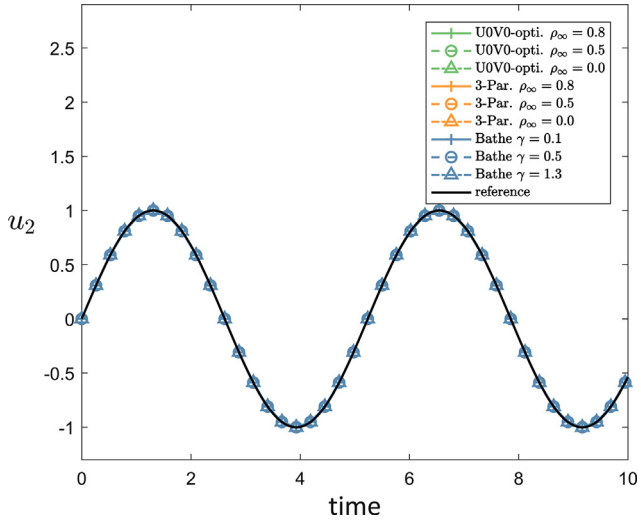

Fig. 7. Displacement of node 2 for various methods The U0V0 method is described in Ref. [5] and the 3-Par. method is described in Refs. [6–8].

of the integration approximation operator of the time integration method.

As the time step size increases, the sign of the real part of each of the eigenvalues, Re$(\lambda_{1,2})$, first changes from positive to negative while the sign of the imaginary part is unchanged. At the point of the sign change of Re$(\lambda_{1,2})$, the first eigenvalue, which rotates counter-clockwise, rotates from the first quadrant to the second quadrant of the complex domain. We then may calculate PE and AD accurately until a certain limit using for $\bar{\Omega}_d > \pi/2$ (as in Ref. [20])

$$\bar{\Omega}_d = \tan^{-1}\left(\sqrt{A_2 - A_1^2}/A_1\right) \tag{35}$$

where $\bar{\Omega}_d = \pi/2$ when the real part of the eigenvalues, A_1, is zero.

However, as the time step size increases further, it reaches the size Δt^* which makes the imaginary part of the eigenvalue become

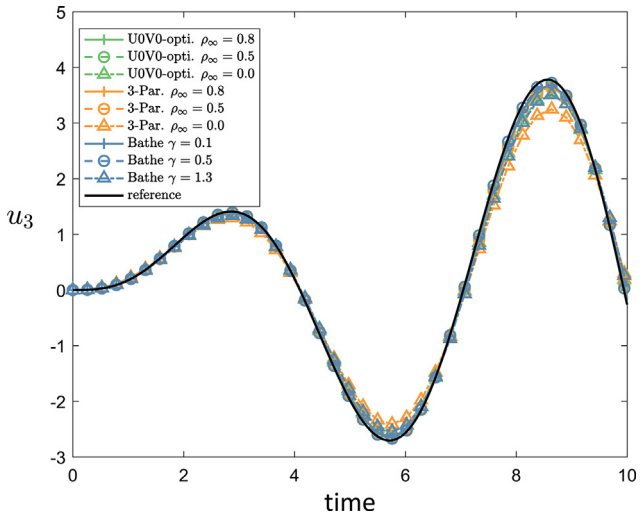

Fig. 8. Displacement of node 3 for various methods.

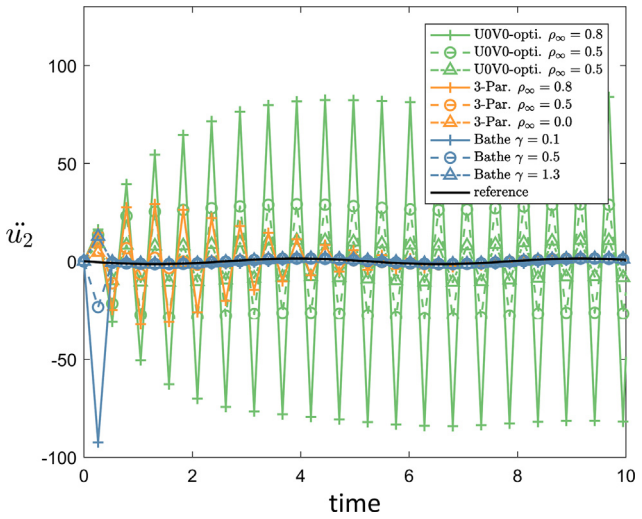

Fig. 11. Acceleration of node 2 for various methods.

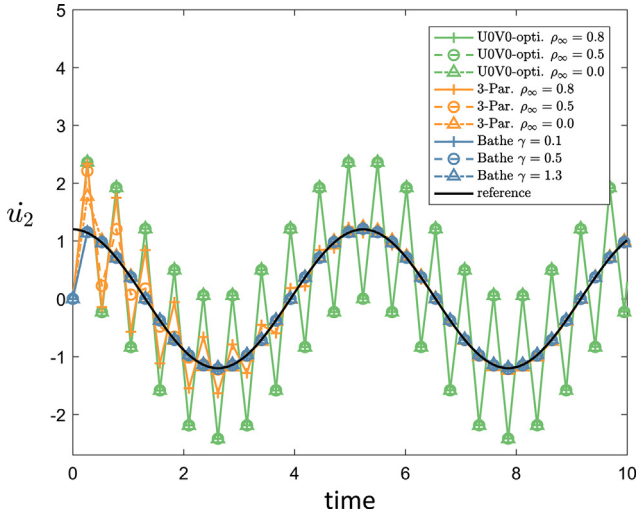

Fig. 9. Velocity of node 2 for various methods (the static correction gives the nonzero velocity at time = 0.0).

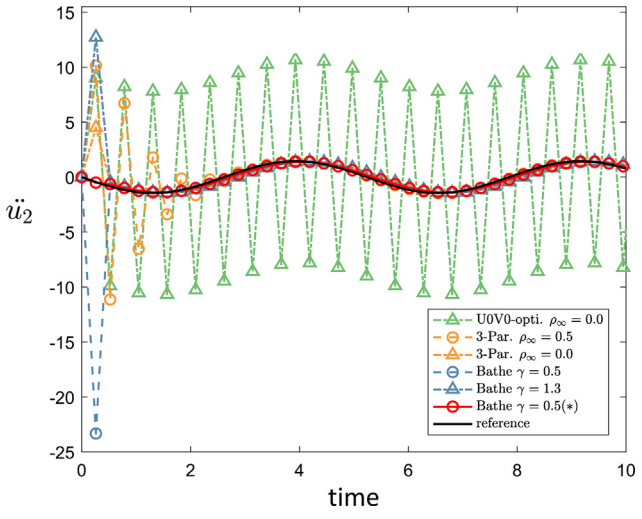

Fig. 12. Acceleration of node 2 for various methods; "Bathe $\gamma = 0.5(*)$" uses $\alpha = 1$ and $\delta = 3/4$ only for the first step, and $\alpha = 1/4$ and $\delta = 1/2$ otherwise.

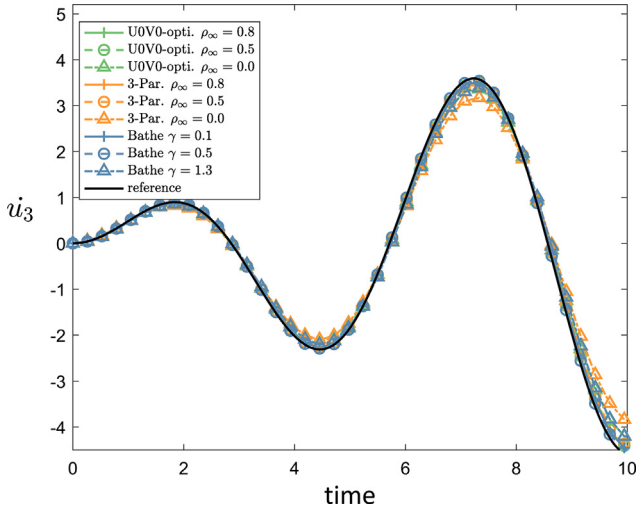

Fig. 10. Velocity of node 3 for various methods.

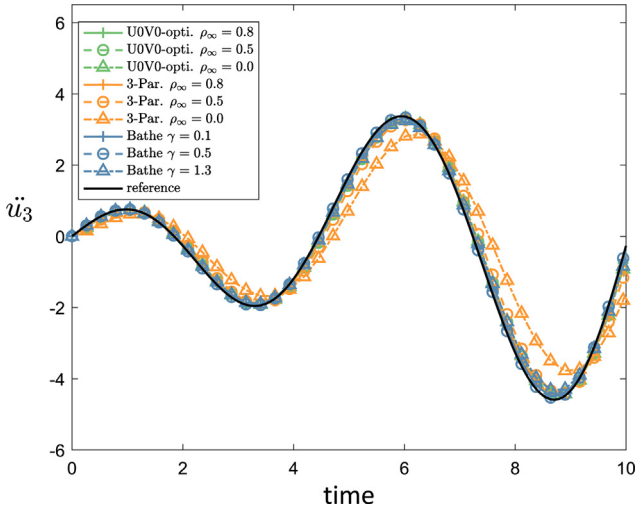

Fig. 13. Acceleration of node 3 for various methods.

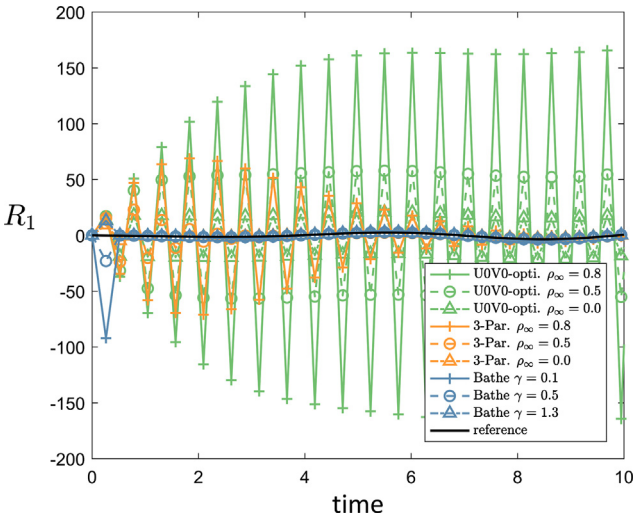

Fig. 14. Reaction force at node 1 for various methods.

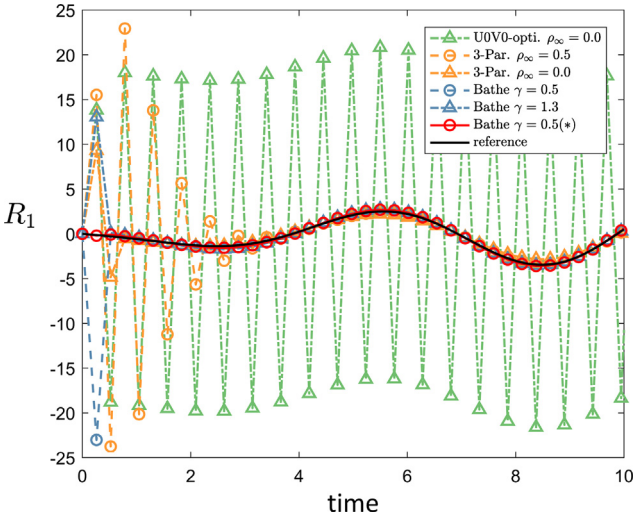

Fig. 15. Reaction force at node 1 for various methods; "Bathe $\gamma = 0.5(*)$" uses $\alpha = 1$ and $\delta = 3/4$ only for the first step, $\alpha = 1/4$ and $\delta = 1/2$ otherwise.

zero, or $A_1^2 = A_2$. For the Bathe method with $\alpha = 1/4, \beta = 1/2$ and $\gamma = 1/2$, $\Delta t^*/T_0 \simeq 0.854$, see Fig. 4c.

Then for the time step size $\Delta t > \Delta t^*$ (since the angle given by Eq. (31) further increases as the time step size increases), if Eq. (35) is used for the PE and AD we obtain an unnatural "kink" in the curves at the time step size Δt^* as shown in Fig. 4a and b. Instead we need to use

$$\bar{\Omega}_d = \begin{cases} \tan^{-1}\left(\sqrt{A_2 - A_1^2}/A_1\right) & \text{for } \Delta t \leqslant \Delta t^* \\ \tan^{-1}\left(-\sqrt{A_2 - A_1^2}/A_1\right) & \text{for } \Delta t > \Delta t^* \end{cases} \tag{36}$$

where $(A_1^2 - A_2)|_{\Delta t = \Delta t^*} = 0$.

To illustrate that we need to use Eq. (36) in our studies of the amplitude decay and period elongation, we solved the single degree of freedom problem

$$\ddot{u} + 100\, u = 0 \tag{37}$$

with the initial conditions $u_0 = 1$ and $\dot{u}_0 = 0$. Fig. 5 shows the numerical solutions using $\alpha = 1/4, \delta = 1/2, \gamma = 1/2$ and various time steps. We see that there is no sudden change in the trend of the numerical solutions around Δt^* as predicted using Eq. (36).

5. Illustrative numerical results

The model problem shown in Fig. 6 was already solved in Ref. [11] to illustrate the behavior of some time integration schemes. We solve the problem here again and include the use of the Bathe method for different values of γ. We refer to Refs. [11,1] for the details of this model problem and comments on its importance.

Figs. 7–15 show the results obtained using the Bathe method, the U0V0$_{\text{optimal}}$ scheme which is a method discussed by Zhou and Tamma as a U0-V0 scheme [5], and the 3 parameter method [6–8]. In all solutions we use $\Delta t = 0.2618$ (as in Ref. [11]). For the Bathe method, we use $\alpha = 1/4$, $\delta = 1/2$ and $\gamma = 0.1, 0.5, 1.3$ while we use various ρ_∞ values for the U0V0$_{\text{optimal}}$ scheme and the 3 parameter method. The results show that the Bathe method performs well with all considered γ values, while the other schemes, for the values of ρ_∞ considered, do not perform satisfactorily.

Note that there is a bifurcation in the principal roots of the characteristic polynomial of the U0V0$_{\text{optimal}}$ scheme at a certain time step size (at the inverted peaks of the curves in Fig. 3(a)). After the bifurcation, the one principal root provides $\rho(\mathbf{A})|_{\Delta t = \infty} \simeq 1$ for all values of ρ_∞ which is the magnitude of the other principal root. Therefore, the U0V0$_{\text{optimal}}$ method does not give the amplitude decay important in the solution of this problem.

The 3 parameter method provides results similar to those of the Newmark method with values for the parameters to give dissipation (see Ref. [11]).

However using the Bathe method, there is an overshoot in the acceleration at node 2 and for the reaction for the first time step. The overshoot is negative for $\gamma \in (0, 1)$ while it is positive for $\gamma > 1$. An analytical study of this behavior shows that this overshoot only occurs in the first step for the given initial conditions, and the overshoot can be eliminated by using $\alpha = 1$ and $\delta = 3/4$ only for the first step.

If we use $\alpha = 1$ and $\delta = 3/4$ only for the first step and $\alpha = 1/4$ and $\delta = 1/2$ thereafter, we have practically the same solutions as for the case of $\alpha = 1/4$ and $\delta = 1/2$ for all solution variables, but without the overshoot. However, we do not recommend to use this set of parameter values for all solution times. With these values only first order accuracy is obtained with large period elongations and amplitude decays, and the algorithm is not unconditionally stable.

6. Concluding remarks

The objective of this paper was to provide some new insight into an implicit time integration method, the Bathe method, for structural dynamics. While the method has already been analyzed in earlier papers, additional insight is given in this paper.

The method was introduced about a decade ago for the solution of structural dynamics problems. In the use of the method and the mathematical analyses, it was assumed that the parameter $\gamma \in (0, 1)$. The analysis we give in this paper shows that using $\alpha = 1/4$ and $\delta = 1/2$ with any real value of γ provides second order accuracy, unconditional stability and good behavior in the principal roots of the approximation operator for all time step sizes. The analysis also shows that the use of $\gamma > 1$ may provide larger amplitude decays, which may be useful in the solution of some problems. The concept of using an enlarged range of the splitting ratio γ might also be valuable in the development of new implicit time integration methods based on a composite strategy.

When analyzing time integration methods, like the Bathe method, for the use of large time steps, it is important to employ

correct measures for period elongations and amplitude decays. We discussed this aspect and used appropriate measures.

In the paper, we focused on the solution of structural dynamics problems. However, the Bathe method shows also valuable accuracy characteristics in the solution of wave propagations, where the technique suppresses waves that can spatially not be resolved and can give increasingly more accurate solutions as the time step size decreases [22,23,25,26]. An analysis of the method for such problem solutions focusing on different values of the parameters δ, α and γ would be very valuable, in particular when used with overlapping finite elements [26]. Finally, the observations given in this paper show that for the design of new composite explicit time integration schemes [27], an enlarged range of the splitting ratio might also be considered.

Acknowledgement

This work was partly supported by the Basic Science Research Program (Grant No. 2017R1C1B5077183) through the National Research Foundation of Korea (NRF) funded by the Ministry of Science and ICT.

Appendix A. The integration operator A and the load operators $\mathbf{L}_a$ and $\mathbf{L}_b$

We give here the expressions for the integration operator **A** and load operators $\mathbf{L_a}$ and $\mathbf{L_b}$:

$$\mathbf{A} = \frac{1}{\beta_1\beta_2}\begin{bmatrix} a_{11} & a_{12} & a_{13} \\ a_{21} & a_{22} & a_{23} \\ a_{31} & a_{32} & a_{33} \end{bmatrix}$$

$$\mathbf{L_a} = \frac{1}{\beta_1\beta_2}\begin{bmatrix} \frac{1}{2}(2\gamma^2\alpha - 4(\alpha-(\delta/2))\gamma - 2\delta)\Omega_0^2 + 2\delta(\gamma-2)\xi\Omega_0 \\ -\gamma(1-\gamma)\alpha\Omega_0^2\Delta t - \delta(\gamma-2)\Delta t \\ 2\gamma(1-\gamma)\alpha\xi\Omega_0\Delta t^2 + \frac{1}{2}(-2\gamma^2\alpha + (4\alpha-2\delta)\gamma + 2\delta)\Delta t^2 \end{bmatrix}$$

$$\mathbf{L_b} = \frac{1}{\beta_1\beta_2}\begin{bmatrix} (\alpha\gamma^2\Omega_0^2 + 2\delta\gamma\Omega_0\xi + 1)(\gamma-2)^2 \\ \Delta t(\gamma-1)(\gamma-2)(\alpha\gamma^2\Omega_0^2 + 2\delta\gamma\Omega_0\xi + 1) \\ \Delta t^2(\gamma-1)^2(\alpha\gamma^2\Omega_0^2 + 2\delta\gamma\Omega_0\xi + 1) \end{bmatrix}$$

where

$$\beta_1 = \alpha\gamma^2\Omega_0^2 + 2\delta\gamma\Omega_0\xi + 1$$

$$\beta_1 = (\gamma-1)^2\Omega_0^2 + 2\xi(\gamma-1)(\gamma-2)\Omega_0 + (\gamma-2)^2$$

$$a_{11} = -2(\Omega_0\xi\gamma(\alpha-\delta/2) + \alpha/2 - 1/4)(\gamma-2)\gamma\Omega_0^2$$

$$a_{12} = -\frac{4(\gamma-2)\Omega_0}{\Delta t}\begin{pmatrix} (1/4)\alpha\gamma^2(\gamma-1)\Omega_0^3 + (1/2)(\gamma^2\alpha + (-2\alpha+\delta)\gamma + \alpha - 2\delta)\xi\gamma\Omega_0^2 \\ +(\gamma-2)(\xi^2\delta\gamma + 1/4)\Omega_0 + (1/2)\xi(\gamma-2) \end{pmatrix}$$

$$a_{13} = -\frac{1}{\Delta t^2}(\gamma-2)\Omega_0^2(\Omega_0^2\alpha\gamma^3 - 2\alpha\gamma^2\Omega_0^2 + 2\Omega_0\delta\gamma^2\xi + \Omega_0^2\alpha\gamma - 4\delta\gamma\Omega_0\xi + \gamma - 2)$$

$$a_{21} = -2\Delta t(\Omega_0\xi\gamma(\alpha-(\delta/2)) + (\alpha/2) - (1/4))\gamma(\gamma-1)\Omega_0^2$$

$$a_{22} = \begin{pmatrix} \Omega_0^2\alpha\gamma^4 + (-4\Omega_0^2\alpha + 2\delta\Omega_0\xi)\gamma^3 + (1 - 2\Omega_0^3\xi(\alpha-\delta) + 4\Omega_0^2\alpha - 8\delta\Omega_0\xi)\gamma^2 \\ +(-4 + 2\Omega_0^3\xi(\alpha-\delta) + \Omega_0^2 + 8\delta\Omega_0\xi)\gamma - \Omega_0^2 + 4 \end{pmatrix}$$

$$a_{23} = -\frac{1}{\Delta t}\Omega_0^2(\gamma-1)(\Omega_0^2\alpha\gamma^3 - 2\alpha\gamma^2\Omega_0^2 + 2\Omega_0\delta\gamma^2\xi + \Omega_0^2\alpha\gamma - 4\delta\gamma\Omega_0\xi + \gamma - 2)$$

$$a_{31} = 4\Delta t^2(\Omega_0\xi\gamma(\alpha-(\delta/2)) + (\alpha/2) - (1/4))\gamma(\xi(\gamma-1)\Omega_0 + (\gamma/2) - 1)$$

$$a_{32} = 4\Delta t\begin{pmatrix} ((1/4)\gamma^2\alpha - (1/2)\alpha\gamma + (\alpha-\delta)\xi^2)\gamma\Omega_0^2(\gamma-1) \\ +(1/2)\Omega_0(\delta\gamma^3 + 1 + (\alpha-4\delta)\gamma^2 + (-2\alpha+4\delta-1)\gamma)\xi + (1/4)(\gamma-2)^2 \end{pmatrix}$$

$$a_{33} = (2\Omega_0\xi(\gamma-1) + \gamma - 2)(\Omega_0^2\alpha\gamma^3 - 2\alpha\gamma^2\Omega_0^2 + 2\Omega_0\delta\gamma^2\xi + \Omega_0^2\alpha\gamma - 4\delta\gamma\Omega_0\xi + \gamma - 2)$$

Appendix B. Supplementary material

Supplementary data associated with this article can be found, in the online version, at https://doi.org/10.1016/j.compstruc.2018.02.007.

References

[1] Bathe KJ. Finite element procedures, 2nd ed. Watertown, MA: K.J. Bathe; 2016. <http://meche.mit.edu/people/faculty/kjb@mit.edu> [also published by Higher Education Press China 2016].
[2] Newmark NM. A method of computation for structural dynamics. J Eng Mech Div (ASCE) 1959;85:67–94.
[3] Wilson EL, Farhoomand I, Bathe KJ. Nonlinear dynamic analysis of complex structures. Int J Earthquake Eng Struct Dyn 1973;1:241–52.
[4] Bathe KJ, Wilson EL. Stability and accuracy analysis of direct integration methods. Int J Earthquake Eng Struct Dyn 1973;1:283–91.
[5] Zhou X, Tamma KK. Design, analysis, and synthesis of generalized single step single solve and optimal algorithms for structural dynamics. Int J Numer Meth Eng 2004;59:597–668.
[6] Shao HP, Cai CW. A three parameters algorithm for numerical integration of structural dynamic equations. Chin J Appl Mech 1988;5(4):76–81 [in Chinese].
[7] Shao HP, Cai CW. The direct integration three-parameters optimal schemes for structural dynamics. In: Proceedings of the international conference: machine dynamics and engineering applications. Xi'an Jiaotong University Press; 1988. p. C16–20.
[8] Chung J, Hulbert GM. A time integration algorithm for structural dynamics with improved numerical dissipation: the generalized-alpha method. J Appl Mech (ASME) 1993;60:371–5.
[9] Bathe KJ, Baig MMI. On a composite implicit time integration procedure for nonlinear dynamics. Comput Struct 2005;83:2513–24.
[10] Bathe KJ. Conserving energy and momentum in nonlinear dynamics: a simple implicit time integration scheme. Comput Struct 2007;85:437–45.
[11] Bathe KJ, Noh G. Insight into an implicit time integration scheme for structural dynamics. Comput Struct 2012;98–99:1–6.
[12] Bathe KJ, Zhang H. Finite element developments for general fluid flows with structural interactions. Int J Numer Meth Eng 2004;60:213–32.
[13] Kroyer R, Nilsson K, Bathe KJ. Advances in direct time integration schemes for dynamic analysis. Automotive CAE Companion 2016/2017; 2016. p. 32–5.
[14] Dong S. BDF-like methods for nonlinear dynamic analysis. J Comput Phys 2010;229:3019–45.
[15] Benítez JM, Montáns FJ. The value of numerical amplification matrices in time integration methods. Comput Struct 2013;128:243–50.
[16] Bathe KJ. Frontiers in finite element procedures & applications. In: Topping BHV, Iványi P, editors. Computational methods for engineering technology. Stirlingshire, Scotland: Saxe-Coburg Publications; 2014 [chapter 1].
[17] Klarmann S, Wagner W. Enhanced studies on a composite time integration scheme in linear and non-linear dynamics. Comput Mech 2015;55:455–68.
[18] Chandra Y, Zhou Y, Stanciulescu I, Eason T, Spottswood S. A robust composite time integration scheme for snap-through problems. Comput Mech 2015;55:1041–56.
[19] Wen WB, Wei K, Lei HS, Duan SY, Fang DN. A novel sub-step composite implicit time integration scheme for structural dynamics. Comput Struct 2017;182:176–86.
[20] Zhang J, Liu Y, Liu D. Accuracy of a composite implicit time integration scheme for structural dynamics. Int J Numer Meth Eng 2017;109:368–406.
[21] Kwon S-B, Lee J-M. A non-oscillatory time integration method for numerical simulation of stress wave propagations. Comput Struct 2017;192:248–68.
[22] Noh G, Ham S, Bathe KJ. Performance of an implicit time integration scheme in the analysis of wave propagations. Comput Struct 2013;123:93–105.
[23] Ham S, Lai B, Bathe KJ. The method of finite spheres for wave propagation problems. Comput Struct 2014;142:1–14.
[24] Belytschko T, Hughes TJR, editors. Computational methods for transient analysis. New York: North-Holland; 1983.
[25] Kim KT, Bathe KJ. Transient implicit wave propagation dynamics with the method of finite spheres. Comput Struct 2016;173:50–60.
[26] Kim KT, Zhang L, Bathe KJ. Transient implicit wave propagation dynamics with overlapping finite elements. Comput Struct 2018;199:18–33.
[27] Noh G, Bathe KJ. An explicit time integration scheme for the analysis of wave propagations. Comput Struct 2013;129:178–93.